Ionization of Anthracene Followed by Fusion in the Solid Phase under Intense Nonresonant Femtosecond Laser Fields†

ARTICLE *in* THE JOURNAL OF PHYSICAL CHEMISTRY C · JULY 2009

Impact Factor: 4.77 · DOI: 10.1021/jp8082985

2 AUTHORS:

Tomoyuki Yatsuhashi
Osaka City University
63 PUBLICATIONS **894** CITATIONS
SEE PROFILE

Nobuaki Nakashima
Toyota Physical and Chemical Institute
211 PUBLICATIONS **4,111** CITATIONS
SEE PROFILE

Ionization of Anthracene Followed by Fusion in the Solid Phase under Intense Nonresonant Femtosecond Laser Fields†

Tomoyuki Yatsuhashi and Nobuaki Nakashima*

Department of Chemistry, Graduate School of Science, Osaka City University, 3-3-138 Sugimoto, Sumiyoshi, Osaka 558-8585, Japan

Received: September 18, 2008; Revised Manuscript Received: December 10, 2008

Fused anthracene cation and a series of anthracene−C_nH_m cluster-like products were observed on irradiation with nonresonant femtosecond pulses at 1.4 μm. Ionization of polycrystalline anthracene revealed strikingly different features such as the absence of multiply charged molecular ions, the appearance of H^+ and C^+ at low intensity without the formation of C_nH_m fragment ions, C_nH_m-attached and detached molecular ions, and multimer cation formation, compared with the gas-phase experiments. The fusion reactions of anthracene and C_nH_m fragments indicated the presence of novel reactions among high-density cations in the crystal produced by femtosecond laser irradiation.

Introduction

The interaction between solid materials and short laser pulse has been widely studied from the perspective of plasma physics, processing of materials,[1] and analytical applications such as matrix-assisted laser desorption ionization.[2] Laser ablation[3] and/or laser desorption have been widely studied and are now used in many applications. However, the main foci of laser ablation studies have been metals, dielectrics, biomaterials, and polymers.[4] Comparison of these results with those of experiments carried out under isolated conditions is quite difficult. However, many experiments have been carried out and many theoretical works have been published regarding the interaction between molecules and high intense laser fields in the gas phase.[5] Because organic molecules in the solid phase are aggregated by van der Waals force, the electronic character of the isolated molecule will be reflected in the physical and chemical processes of the solid. Comparing the results in the solid phase with those in the gas phase will provide fruitful information toward understanding the molecular mechanism in the solid phase. Although burst experiments have been carried out for laser ablation, there are some important problems that have been left unsolved or have not been examined well. First, most of the laser ablation processes have been induced by resonant excitation of materials. The nanosecond UV resonant laser ablation of organic molecules was examined in polymer films,[6] neat liquid,[7] and solutions.[8] Nanosecond and femtosecond UV resonant ablation of neat benzene derivatives gave important information about the molecular mechanism of ablation.[9] The morphological changes during ablation processes were monitored by time-resolved shadowgraph techniques, and the time scale of plume formation was characterized. The time-resolved absorption spectra revealed the presence of electronically excited states and neutral radicals as intermediates during ablation processes. Photothermal (heating by the relaxation of excited states followed by melting and boiling) and photochemical (expand the bulk by the formation of radicals and low molecular weight gases) mechanisms were proposed as the origin of ablation. For femtosecond resonant studies, morphological changes such as the fracture and destruction of anthracene microcrystals on a quartz substrate (threshold ~40 mJ cm^{-2}) have been observed under the microscope (resonant, 390 nm, 150 fs).[10] On the other hand, few studies have been carried out regarding femtosecond nonresonant ablation of organic solids. Multistep discrete etching has been achieved by two-photon ablation of amorphous organic film (780 nm, 150 fs).[11] Nonresonant excitation results in the degradation of anthracene microcrystal (1260 nm, 35 fs, 100 kHz, >2 nJ/pulse) under the microscope.[12] We recently examined the desorption of C_{60}^+ from a solid ionized by nonresonant wavelength of both neutral and cationic states.[13] We proposed that the desorption of molecular ion was driven by Coulomb explosion[14] (electrostatic mechanism). The advantages of nonresonant femtosecond excitation were identified in the intact ion formation[15] in addition to highly charged molecular ion formation[16] in the gas phase. We found factors key to the formation of intact molecular ions such as wavelength, pulse duration, and polarization.[17] The key issue is that fragmentation is enhanced when the cation radical exhibits absorption at the laser wavelength although ion was formed by the nonresonant ionization process of neutral. To avoid the complexity that arises from postionization processes initiated by photoabsorption of the cation radical,[18] as well as from substrate heating and/or ionization processes, we used the nonresonant femtosecond laser both for neutral and cation, a thick organic layer, and a transparent substrate to investigate the molecular mechanism of ionization and desorption of molecules.

Second, ablation processes have been primarily argued by fluence (mJ cm^{-2}, the number of photons) scale; however, the interaction between molecules and intense electric fields should be discussed with regard to intensity (W cm^{-2}, the number of photons per unit time) because nonresonant multiphoton ionization is a nonlinear process and the tunneling ionization depends on the strength of the laser electric fields. The fluence scale is suitable for discussing thermal (quasi static) processes. The pulse width (56 fs) used in this study is sufficiently short and initiated a multiphoton (tunneling) process, so the fluence scale was not suitable. Generally speaking, ionization should take place above 10^{13} W cm^{-2} in the case of organic molecules. We examined

† Part of the "Hiroshi Masuhara Festschrift".

* To whom correspondence should be addressed. E-mail: nakashim@sci.osaka-cu.ac.jp. Phone: +81-6-6605-2552. Fax: +81-6-6605-2522.

10.1021/jp8082985 CCC: $40.75
Published on Web 01/26/2009

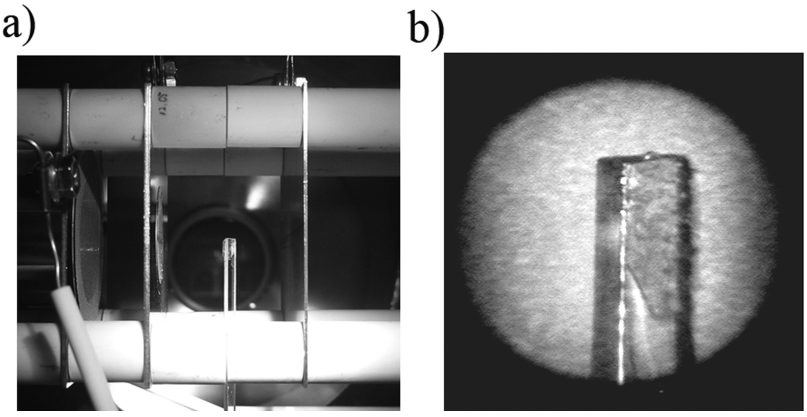

Figure 1. (a) Photograph of an acceleration region for a time-of-flight mass spectrometer. The laser beam comes from the opposite side. Polycrystalline anthracene on the quartz plate is inserted between the two electrodes. (b) Telescope image of an irradiated surface of polycrystalline anthracene on a quartz substrate. The quartz substrate is in 2 mm width, and 1 mm thickness, thus, the incident angle of 45° can be confirmed by the ratio (2:1) of the projection width of them.

femtosecond nonresonant (both for neutral molecules and cations) ionization of anthracene solid in this study.

Third, although the complexities of physical and chemical processes during ablation such as photoexcitation, annihilation of excited states, bond-breaking, heating by internal conversion,[19] melting, and ejection of molecules[20] are generally known, chemical reactions other than bond dissociation in ablated plumes or on solid surfaces have not been discussed, despite the success of fullerene investigations.[21] The synthesis of materials by laser ablation techniques has been limited to nanoparticles, inorganic materials, and films (deposition, coating, implantation). One of the reasons for this limitation is that the qualitative analysis of ablated materials is difficult by photospectroscopy and microscopes. Ion detection is one of the important methods of achieving qualitative analysis of ablated materials; however, the detection of ions has rarely been examined. We found that fusion of the molecular ion and the attachment of fragments to the molecular ion can possibly be applied as a novel preparation method for new materials.

Experimental Methods

A piece of polycrystalline anthracene (Aldrich, 99%) was attached to a quartz plate with a polymer-based glue. The thickness of the crystal was typically 200 μm. Details of the ionization experiments have been described elsewhere.[22] Briefly, the ion generated by focusing laser light was analyzed by a homemade Wiley−McLaren-type dual extraction stage time-of-flight mass spectrometer with resolution ($m/\Delta m$, fwhm) of 500 at m/z 129 for xenon. An aperture of 6 mm diameter was located on the extraction plate. The base pressure of both the ionization and time-of-flight chambers was below 5×10^{-7} Pa. The pressure during the anthracene experiments was below 10^{-5} Pa. A thin sample plate was inserted in the acceleration region (Figure 1), and hence the ion optics were optimized to correct the distortion of the electrostatic field. The acceleration voltage was 3000 V, and an extraction field potential of 625 V cm^{-1} was applied. The sample plate was moved to the shooting laser beam on the fresh surface. A 45-fs pulse from a 0.5 TW all-diode-laser-pumped Ti:Sapphire laser system (Thales laser, alpha 100/XS, 100 Hz, >15 mJ, 800 nm) was used to pump an optical parametric amplifier (Quantronix, TOPAS 4/800). The pulse width was measured with a second-order scanning autocorrelator (APE, PulseCheck). The same optical elements, including the ionization chamber window, focusing lens, beam splitter, and neutral density filters, were placed in front of the autocorrelator to create the same group velocity dispersion. A pulse of 56 fs (fwhm) duration at 1.4 μm was used for the experiments. The direction of the laser polarization was orthogonal to the time-of-flight axis. The laser beam was focused onto anthracene with an incident angle of 45° with use of a plano-convex quartz lens with a focusing length of 300 mm. The incident angle was confirmed by the telescope image (Figure 1). The actual laser intensity at the focus was determined by measuring the saturation intensity of xenon by the method of Hankin et al.[23] The output signal from an MCP (Burle, APTOF25) was averaged by a digital oscilloscope (LeCroy, Waverunner 6050A, 500 MHz) and the ion yield was obtained by integrating over the appropriate peak in the time-of-flight spectrum.

Results and Discussion

Desorption of Ions. Figure 2 shows the time-of-flight mass spectra of polycrystalline anthracene. As shown in Figure 2a, anthracene ion (M^+) accompanying H^+ and C^+ appeared without forming heavier fragments. M_2^+ could also be identified at the lowest intensity of ion detection. H^+ and C^+ production by the dissociation and ionization of H and C was not considered because the pulse duration of the laser is much shorter than the time scale of the dissociation process of neutral fragments. The fragmentation from a heavier ion forming H^+ would be possible, but it would be less possible for C^+. The origins of C^+ emissions were likely not an ordinary chemical bond-breaking reaction of a heavier fragment ion. It is interesting that the peaks of H^+ and C^+ were split even at low intensity. The double peaks (Figure 2d) indicate the spatial distribution of ions originating in the geometrical configuration of laser irradiation. In addition, the splitting of CH_m^+ ($m = 0, 1, 2, 3$) and $C_2H_m^+$ ($m = 0, 1$) was also observed but heavier fragments showed single peaks. The relationships among the degree of split, applied voltage, incident angle of the laser beam, laser polarization, and laser intensity are interesting. Fragmentation, M_2^+ and M_3^+ formation, and C_nH_m attachments to and detachments from M^+ and M_2^+ were visible at higher intensities (Figure 2b). Due to the broadness of the ion peaks, it was not clear whether M^+ ($\Delta m = 4.8$, fwhm) and M_2^+ ($\Delta m = 7.7$, fwhm) were composed of a single molecular ion peak or of hydrogen attached or lost peaks. The resolutions of mass spectra were 40−60 in the entire region; we can therefore distinguish hydrogen attached to carbon when the carbon number is smaller than 5. Ions consisting of more than 6 carbon atoms showed a broad distribution. Although the peaks were broad, they were separated by 12, and we

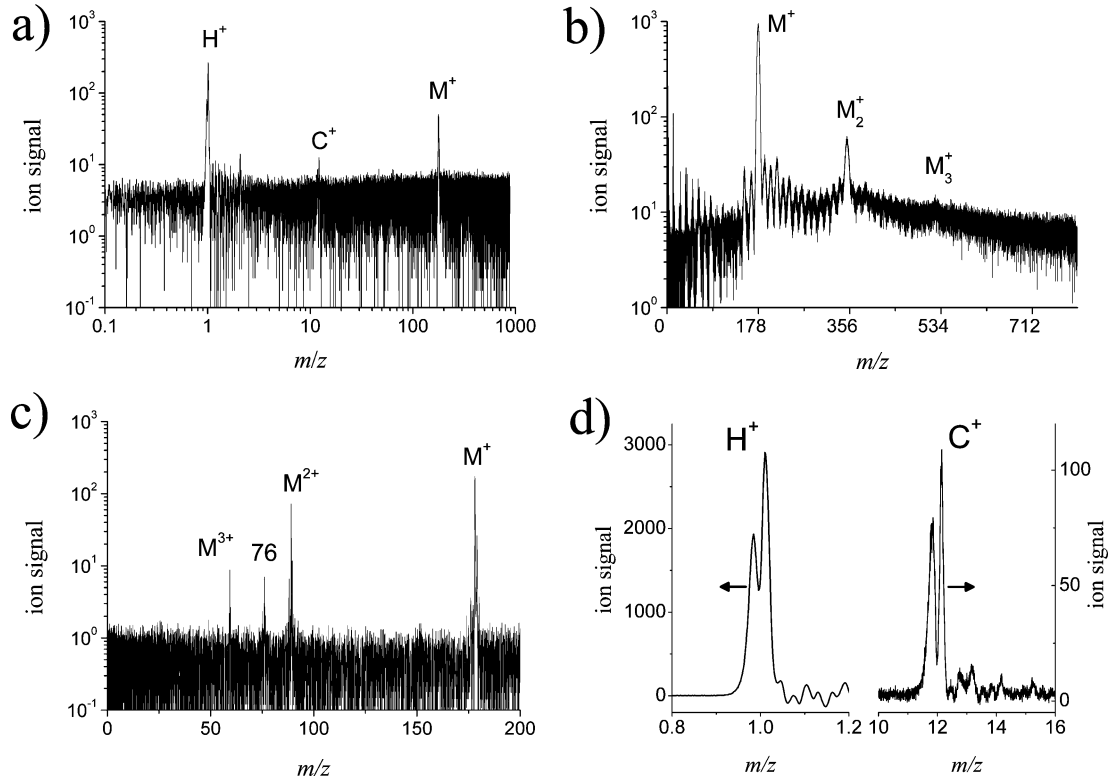

Figure 2. Time-of-flight mass spectra of solid anthracene ionized with 1.4-μm pulses of 56 fs at (a) 4.5×10^{12} and (b) 10×10^{12} W cm^{-2}. The base signal was not subtracted. M^+, M_2^+, and M_3^+ denote the monomer, dimer, and trimer of molecular ions, respectively. (c) Time-of-flight mass spectrum of anthracene in the gas phase ionized with 1.4-μm pulses of 130 fs at 5.0×10^{13} W cm^{-2}. M^+, M^{2+}, and M^{3+} denote the singly, doubly, and triply charged molecular ions, respectively. Data were taken from ref 25 and were replotted on a logarithmic scale. Reprinted with permission from Elsevier (ref 25). (d) The same mass spectra of b. The spectra of hydrogen and carbon ions are magnified.

identified the carbon number up to 42 at 10×10^{12} W cm^{-2}. To our knowledge, only the femtosecond laser pulse which resonates with cationic state resulted in significant fragmentation in the gas phase.[24] Attachment, detachment, and multimer formation appear to be the most important characteristics in the solid phase and should be key clues for clarifying molecular processes.

Contrary to the results of gas-phase experiments, multiply charged ions were entirely absent in the ionization of solid anthracene on a quartz substrate. This absence was also true for C_{60} even at 10^{14} W cm^{-2} (0.8 μm).[13] Usually, the peak of multiply charged ions is quite sharp and easily identified with the help of an accompanying isotope peak appearing at the noninteger number. Highly charged molecular ions have been commonly observed from many organic systems by femtosecond laser irradiation in the gas phase.[16] We observed multiply charged anthracene and also naphthalene up to 3+ with little fragmentation by 1.4 μm pulse (130 fs) in the gas phase[25] as shown in Figure 2c. It is obvious that light fragments such as H^+ and C^+ were not observed at all under isolated conditions. It was clear that the presence of H^+ and C^+ without the formation of heavier fragment ions at low intensity provided strikingly different features of the solid phase compared with the gas phase experiments. Considering the laser intensity used in this study and the lowering ionization potential in the solid phase, highly charged molecular ions must initially be formed by 1.4 μm pulse irradiation even in the solid phase. The desorption mechanism would be the same as that postulated in the case of C_{60}.[13] Once highly charged anthracene was formed, redistribution of charges was presumably completed in a very short time because of the high density of the solid. Gas-phase experiments have been carried out under a typical pressure of 5.0×10^{-5} Pa, which corresponds to 2.0×10^{-11} M; therefore, charge redistribution is not possible. In contrast, the concentration of anthracene in the solid phase is 7.0 M (1.25 g cm^{-3}), and thus hole neutralization by neighboring neutral anthracene would take place immediately, finally resulting only in anthracene cation formation. Singly charged anthracene was emitted by a Coulomb explosion due to the high density of the anthracene ion produced. C^+ would also be emitted by Coulomb explosion, probably due to the temporal charge localization[26] within the framework of anthracene.

Figure 3 shows the laser-intensity dependence of anthracene ion yields. The slopes below 10×10^{12} W cm^{-2} indicated in Figure 3 are 7. The ion yield of M^+ saturated above 10×10^{12} W cm^{-2} and the slopes of 1.5 are also indicated. The saturation behavior would be explained by the expansion of high-intensity volume as the laser intensity increased because the ionization probability became unity at a certain intensity. Suppose that the intensity of the laser beam had a Gaussian distribution in space and the detection of ions was not restricted by a slit, the slope would be 1.5.[27] Recombination of cation and electron could be the reason of saturation behavior; however, the slope of 1.5 may be too shallow. Saturation due to the fragmentation of M^+ at high intensity was not appropriate because the ion yields of H^+, C^+, and M_2^+ were also saturated at the same intensity. We therefore concluded that all molecules were ionized at the laser-focused surface above 10×10^{12} W cm^{-2}. The highly dense cation was formed on the surface of a very small area and finally ejected to the vacuum by Coulomb repulsion force.

Ionization Mechanism. The nonresonant multiphoton and tunnel ionization rate was primarily dominated by the ionization potential. The ionization potentials of organic solids have been

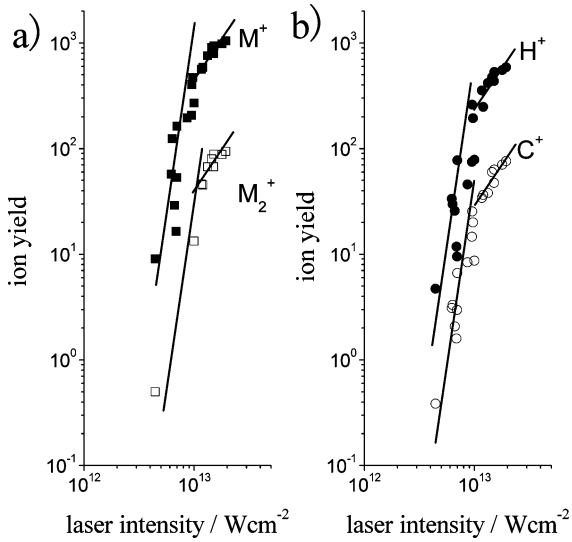

Figure 3. Ion yields of anthracene (solid square), dimer (open square), H^+ (solid circle), and C^+ (open circle) as a function of laser intensity. M^+ and M_2^+ denote the monomer and dimer of molecular ions. The solid lines have slopes of 7 (lower than 10×10^{12} W cm^{-2}) and 1.5 (higher than 10×10^{12} W cm^{-2}).

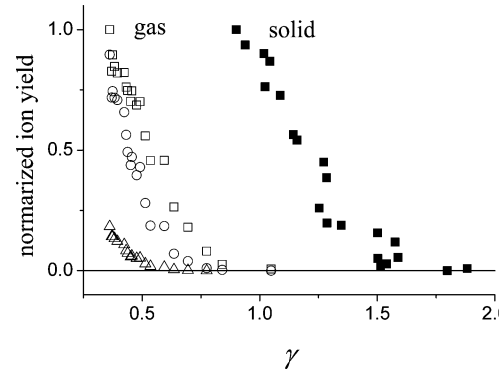

Figure 4. Ion yields as a function of the Keldysh adiabaticity parameter γ. Singly (open square), doubly (open circle), and triply (open triangle) charged molecular ions observed in the gas phase (130 fs, 1.4 μm). Singly charged molecular ion (solid square, 56 fs, 1.4 μm) observed in the solid phase.

studied in detail by Sato et al.[28] The vertical and adiabatic ionization potentials of anthracene are 7.40 and 7.36 eV in the gas phase, while threshold (bulk) and peak (near to the surface) ionization potentials of solid anthracene are 5.70 and 6.4 eV, respectively.[28] Some difference has also been reported in threshold ionization potentials between single crystal (5.67 eV) and polycrystalline (5.75 eV) states.[29] If we take the latter value into account, 7 (6.5) photons of a 1.4 μm pulse (0.89 eV) are necessary to ionize anthracene. The Keldysh adiabaticity parameter γ defines the border between the multiphoton ionization and the tunnel ionization regime of atoms,[30] and the tunnel ionization mechanism dominates when γ is much smaller than unity. In contrast, the conventional Keldysh parameter based on the Coulomb model and zero-range potential model was concluded to underestimate the border between the multiphoton-ionization and tunneling-ionization regimes in the cases of large molecules. The existence of tunneling ionization has been reported at larger γ values in the case of large molecules[31] in the gas phase and even in the cases of liquid rare gas.[32] Suppose the ionization potential is 5.75 eV, γ is 1.3 at 10×10^{12} W cm^{-2} (1.4 μm). It is concluded that both tunneling and multiphoton ionization mechanisms may be involved under our experimental conditions, although a simple and fundamental question remained. Figure 4 compares ion yields of molecular ions obtained in the gas and solid phase experiments as a function of γ. Although we took the difference of ionization potentials into accounts, singly charged molecular ion was observed at larger γ values in the case of solid. It would be a challenging problem for high intense laser field chemistry whether we could use γ in the case of organic solid or not.

There may be another possible ionization mechanism such as the annihilation of the electronically excited states,[33] and further excitation of the electronically excited state.[34] The first mechanism will be excluded because ionization took place in the gas phase where the bimolecular reaction was impossible at the pressure used in the previous study. To excite anthracene to its S_1 state (3.1 eV), 4 (3.5) photons are necessary in the solid phase. In both the solid and liquid phases, the ionization potential became lower than in the gas phase due to the stabilization. As a result, the energy gap between the lowest excited state and the continuum level became closer. In the case of anthracene, the difference is 2.7 eV (3.0 photons) in the solid phase and 4.1 eV (4.6 photons) in the gas phase. The transition from S_1 state to continuum was expected to be much easier in the solid phase than in the gas phase. We observed blue emissions below 2.8×10^{12} W cm^{-2} where we cannot observe ions; however, the second mechanism will be neglected by calculating the tunneling ionization rate for the formation of M^+. The ionization rate became much faster (tunneling regime) as we increased the laser intensity. The tunnel ionization probability was calculated to be unity above 8.6×10^{12} (56 fs, 5.75 eV, solid) and 1.9×10^{13} W cm^{-2} (130 fs, 7.4 eV, gas), respectively.[35] At 10×10^{12} W cm^{-2}, the tunnel ionization rate (56 fs, 5.75 eV, solid) was estimated to be 8.8×10^{14} s^{-1} (1.1 fs). When the laser intensity was low, the ionization rate was very slow, allowing the excited state formation. For example, the ionization rate was 1.6×10^{11} s^{-1} (6.4 ps) at 2.8×10^{12} W cm^{-2} (56 fs, 5.75 eV, solid) where we observed blue emissions but did not observe ions.

Attachments, Detachments, and Fusion of Molecular Ions. The results for anthracene can be compared with those of direct ionization/desorption experiments by free electron lasers (FEL, 7.7 μm, 2 μs, NaCl substrate).[36] They prepared a 100-μm thick layer of anthracene by depositing toluene solution followed by drying. It was quite interesting that they did not observe coalescence, wavelength dependence but observed small fragmentation, C_nH_m attachments to M^+ ($n < 6$), detachment from M^+ ($n < 3$), delayed ionization, and white plasma emissions. The absence of coalescence and the presence of delayed ionization was different from our results. It should be noted that the similar FEL experiments gave different results.[37] The major ions generated by 7.6-μm pulse (2 μs, 4 J cm^{-2}) were C_2^+, $C_3H_3^+$, and a small amount of M^+ accompanying a broad plasma emission. Ion emissions were observed after the induction period (more than 1000 laser shots at 9 J cm^{-2}), where graphite-like species that absorbed photons more efficiently than intact anthracene were formed. They concluded that the intact anthracene was not ionized by FEL but that graphite-like species generated plasmas and anthracene ion was formed in the gas phase (plasma) after thermal ejection of the neutral molecules from the solid surface. The reason for the contradictions in their two experiments remains unclear, but they may perhaps be due to the difference in laser fluence. A burst of infrared laser pulses can ionize molecules by thermal processes and thermal decomposition would dominate as the laser fluence and the number of pulses was increased. It is important to note that they observed

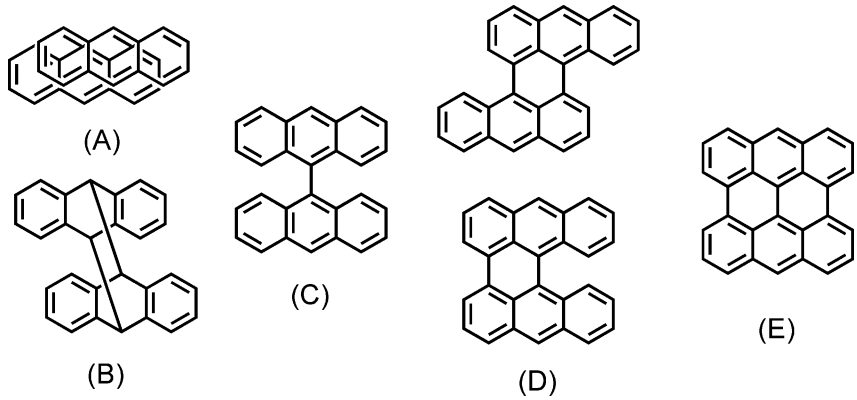

Figure 5. The possible structures of the anthracene dimer cation (M_2^+): (A) π-dimer cation; (B) anthracene photodimer; (C) 9,9′-bianthracene; (D) dibenzo[*a*,*j*]perylene, dibenzo[*a*,*o*]perylene; and (E) phenanthro[1,10,9,8-opqra]perylene.

the coalescence of C_{60}, but not for anthracene, in the preceding study.[36] In contrast, we observed the coalescence (M_2^+ formation) in both C_{60}[13] and anthracene. The intensity dependences of M^+ and M_2^+ were the same for two molecules; however, the shape of the M_2^+ peak was very different (Figure 2b). M_2^+ of C_{60} showed a very broad peak ($\Delta m \approx 200$, resolution was 7.2), whereas Δm of anthracene M_2^+ was 7.6 (resolution was 46) at 10×10^{12} W cm^{-2}. We postulated that $(C_{60})_2^+$ is formed away from the surface by the collision of ions thermally emitted from the surface and neutrals at the wing of the focus spot where they remain, giving a mass peak with broad distribution. The resolutions of all ions from anthracene were similar (40−60) and we cannot observe the tailing component of M^+ that originated in the delayed (thermal) ionization observed in C_{60}.[13] Those results indicated that all ions were exposed to similar heating processes and that their birth places were similar. Thus, M^+ formed by tunneling ionization at the surface presumably fused with the neutral molecule in the bulk, resulting in dimer cation formation and giving a mass peak that was less broad than that of $(C_{60})_2^+$.

Fragmentation, attachments, detachments, and fusion reactions were triggered by femtosecond laser irradiation. The dominant product was a kind of dimer cation rather than attached or detached products. The above reactions should occur thermally and the thermal energy could be formed by the following processes: the neutralization of highly charged anthracene by neighboring molecules, a conformational change through the charge transfer process, the electron−hole recombination, and electrons penetration into the bulk. As a result of releasing considerable energy to the lattice, fragmentation, attachments, detachments, and fusion occurred in the solid phase. It is notable that previously reported C_{60}[13] is a somewhat special molecule due to its stability in multiply charged states[38] and its large dissociation energy. C_{60} could accumulate energy as a heat-bath and showed delayed ionization; however, the dissociation energy of anthracene is smaller than that of C_{60}, and thermal fragmentation would proceed easily and not show delayed ionization.

There would be a small possibility of photoinduced fragmentation of the anthracene cation radical at 1.4 μm excitation because anthracene cation is transparent at the laser wavelength. However, photoinduced decomposition of a dimer cation would occur if the dimer cation was produced during the laser pulse and had strong absorption at the laser wavelength of 1.4 μm. Although the bimolecular reaction would not complete within 56 fs even in the condensed media, it is worth considering the effect of photodecomposition of produced dimer cations because the effects of resonantly induced fragmentation of cation were investigated in the gas phase even for a 40-fs pulse.[39] The absorption of anthracene π-dimer cation appeared at the shorter[40] and longer[41] wings of monomer cation absorption,[42] which were centered at around 700−800 nm in solution and in a rigid matrix. Absorption of π-dimer cation in the near-infrared region ($\lambda_{max} > 1.6$ μm) was reported for 9-bromoanthracene in rigid matrix at 77 K.[43] The absorption maximum of π-dimer anion located at 1.8 μm[44] and the similarity of cation and anion spectra could indicate that the absorption band in the near-infrared region also exists in the case of unsubstituted anthracene π-dimer cation. However, the same laser intensity dependence between monomer and dimer ions indicated the absence of photoinduced fragmentation of dimer. Thus, the possibility of a π-dimer cation was excluded. The basic question about the structure of the dimer cation was left unsolved. A covalently linked anthracene may be a candidate because the kinetic energy of the ion was large. The binding energy of observed dimer cation should be larger than the internal energy. The peak width (fwhm) of M^+ at 4.5×10^{12} W cm^{-2} was equivalent to the kinetic energy distribution of about 9.2 eV. The possibility of dianthracene (anthracene photodimer) was excluded because of its small enthalpy of dissociation (0.30 eV).[45]

We cannot determine the precise mass of the dimer cation due to low resolution; therefore, the dimer cation would not necessarily be $C_{28}H_{20}$, but would be at least $C_{28}H_m$. The candidates would be linked cations such as bianthracene (2H loss) and/or fused cations such as dibenzoperylene (4H loss) and phenanthroperylene (6H loss) produced by coalescence[46] as shown in Figure 5.

To better our understanding of the reactions in the solid phase, it is necessary to identify the dimer structure as well as the crystal morphology before and after laser irradiation, and the relationship among emissions (fluorescence, plasma, blackbody), ions (molecular, fragment, multimer), and laser intensity. This information will provide us with fruitful information about the whole mechanism including excited states, continuum, and plasma. We are now examining mixed crystals to induce intermolecular reactions by femtosecond laser pulses.

Acknowledgment. The present research was partially supported by a Grant-in-aid from the Ministry of Education, Culture, Sports, Science and Technology, Japan.

References and Notes

(1) Bäuerle, D. *Laser Processing and Chemistry*; Springer: Berlin, Germany, 2000.

(2) Karas, M.; Hillenkamp, F *Anal. Chem.* **1988**, *60*, 2299. Tanaka, K.; Waki, H.; Ido, Y.; Akita, S.; Yoshida, Y.; Yoshida, T. *Rapid Commun. Mass Spectrom.* **1988**, *2*, 151–153.

(3) Kawamura, Y.; Toyoda, K.; Namba, S. *Appl. Phys. Lett.* **1982**, *40*, 374. Srinivasan, R.; Leigh, W. J. *J. Am. Chem. Soc.* **1982**, *104*, 6784.
(4) Srinivasan, R.; Braren, B. *Chem. Rev.* **1989**, *89*, 1303.
(5) Nakashima, N.; Shimizu, S.; Yatsuhashi, T.; Sakabe, S.; Izawa, Y. *J. Photochem. Photobiol. C* **2000**, *1*, 131. Levis, R. J.; DeWitt, M. J. *J. Phys. Chem. A* **1999**, *103*, 6493.
(6) Fujiwara, H.; Fukumura, H.; Masuhara, H. *J. Phys. Chem.* **1995**, *31*, 11844. Fujiwara, H.; Hayashi, T.; Fukumura, H.; Masuhara, H. *Appl. Phys. Lett.* **1994**, *64*, 2451.
(7) Tsuboi, Y.; Hatanaka, K.; Fukumura, H.; Masuhara, H. *J. Phys. Chem.* **1994**, *44*, 11237.
(8) Hatanaka, K.; Kawano, M.; Tsuboi, Y.; Fukumura, H.; Masuhara, H. *J. Appl. Phys.* **1997**, *82*, 5799.
(9) Hatanaka, K.; Tsuboi, Y.; Fukumura, H.; Masuhara, H. *J. Phys. Chem. B* **2002**, *106*, 3049.
(10) Hosokawa, Y.; Mito, T.; Tada, T.; Asahi, T.; Masuhara, H. *RIKEN Rev.* **2002**, *43*, 35. Hosokawa, Y. Thesis, Osaka University, 2000.
(11) Hosokawa, Y.; Yashiro, M.; Asahi, T.; Masuhara, H.; Kadota, T.; Shirota, Y. *Jpn. J. Appl. Phys.* **2001**, *40*, L1116.
(12) Matsuda, H.; Fujimoto, Y.; Ito, S.; Nagasawa, Y.; Miyasaka, H.; Asahi, T.; Masuhara, H. *J. Phys. Chem. B* **2006**, *110*, 1091. Matsuda, H. Thesis, Osaka University, 2006.
(13) Yatsuhashi, T.; Nakashima, N. *J. Phys. Chem. A* **2008**, *112*, 5781.
(14) Shimizu, S.; Zhakhovskii, V.; Sato, F.; Okihara, S.; Sakabe, S.; Nishihara, K.; Izawa, Y.; Yatsuhashi, T.; Nakashima, N. *J. Chem. Phys.* **2002**, *117*, 3180. Shimizu, S.; Zhakhovskii, V.; Murakami, M.; Tanaka, M.; Yatsuhashi, T.; Okihara, S.; Nishihara, K.; Sakabe, S.; Izawa, Y.; Nakashima, N. *Chem. Phys. Lett.* **2005**, *404*, 379.
(15) DeWitt, M. J.; Levis, R. J. *J. Chem. Phys.* **1995**, *102*, 8670.
(16) Ledingham, K. W. D.; Singhal, R. P.; Smith, D. J.; McCanny, T.; Graham, P.; Kilic, H. S.; Peng, W. X.; Wang, S. L.; Langley, A. J.; Taday, P. F.; Kosmidis, C. *J. Phys. Chem. A* **1998**, *102*, 3002.
(17) Nakashima, N.; Yatsuhashi, T. In *Progress in Ultrafast Intense Laser Science II*; Yamanouchi, K., Chin, S. L., Agostini, P., Ferrante, G., Eds.; Springer: Berlin, Germany, 2007; p 25.
(18) Harada, H.; Shimizu, S.; Yatsuhashi, T.; Sakabe, S.; Izawa, Y.; Nakashima, N. *Chem. Phys. Lett.* **2001**, *342*, 563. Harada, H.; Tanaka, M.; Murakami, M.; Shimizu, S.; Yatsuhashi, T.; Nakashima, N.; Sakabe, S.; Izawa, Y.; Tojo, S.; Majima, T. *J. Phys. Chem. A* **2003**, *107*, 6580. Trushin, S. A.; Fuss, W.; Schmid, W. E. *J. Phys. B* **2004**, *37*, 3987. Wu, D.; Wang, Q.; Cheng, X.; Jin, M.; Li, X.; Hu, Z.; Ding, D. *J. Phys. Chem. A* **2007**, *111*, 9494. Pearson, B. J.; Nichols, S. R.; Weinacht, T. *J. Chem. Phys.* **2007**, *127*, 131101.
(19) Fukumura, H.; Masuhara, H. *Chem. Phys. Lett.* **1994**, *221*, 373.
(20) Fukumura, H.; Kohji, Y.; Nagasawa, K.; Masuhara, H. *J. Am. Chem. Soc.* **1994**, *116*, 10304.
(21) Kroto, H. W.; Heath, J. R.; O'Brien, S. C.; Curl, R. F.; Smalley, R. E. *Nature* **1985**, *318*, 162.
(22) Yatsuhashi, T.; Obayashi, T.; Tanaka, M.; Murakami, M.; Nakashima, N. *J. Phys. Chem. A* **2006**, *110*, 7763.
(23) Hankin, S. M.; Villeneuve, D. M.; Corkum, P. B.; Rayner, D. M. *Phys. Rev. A* **2001**, *64*, 013405.
(24) If the ion has a repulsive potential energy surface, there is no chance for the molecular ion to survive.
(25) Murakami, M.; Mizoguchi, R.; Shimada, Y.; Yatsuhashi, T.; Nakashima, N. *Chem. Phys. Lett.* **2005**, *403*, 238. Yatsuhashi, T.; Nakashima, N *J. Phys. Chem. A* **2005**, *109*, 9414.
(26) Yatsuhashi, T.; Murakami, M.; Nakashima, N. *J. Chem. Phys.* **2007**, *126*, 194316.
(27) Posthumus, J. H.; McCann, J. F. In *Molecules and Clusters in Intense Laser Fields*; Posthumus, J., Ed.; Cambridge University Press: Cambridge, UK, 2001; p 27.
(28) Sato, N.; Seki, K.; Inokuchi, H. *J. Chem. Soc., Faraday Trans. 2* **1981**, *77*, 1621. Sato, N. In *Electrical and Related Properties of Organic Solids*; Munn, R. W., Miniewicz, A., Kuchta, B., Eds.; Springer: Dordrecht, The Netherlands, 1997; p 157.
(29) Schmid, B. M.; Sato, N.; Inokuchi, H. *Chem. Lett.* **1983**, 1897. Sato, N.; Inokuchi, H.; Schmid, B. M.; Karl, N. *J. Chem. Phys.* **1985**, *83*, 5413.
(30) Keldysh, L. V. *Sov. Phys. JETP* **1965**, *29*, 1307.
(31) DeWitt, M. J.; Levis, R. J. *J. Phys. Rev. Lett.* **1998**, *23*, 5101.
(32) Pettersson, M.; Zadoyan, R.; Eloranta, J.; Schwentner, N.; Apkarian, V. A. *J. Phys. Chem. A* **2002**, *106*, 83080.
(33) Silver, M.; Olness, D.; Swicord, M.; Jarnagin, R. C. *Phys. Rev. Lett.* **1963**, *10*, 12.
(34) Choi, S.-I. *J. Chem. Phys.* **1964**, *40*, 1691.
(35) Ammosov, M. V.; Delone, N. B.; Krainov, V. P. *Sov. Phys. JETP* **1986**, *641*, 1191.
(36) Hamada, Y.; Kondoh, H.; Ogawa, Y.; Tono, K.; Ohta, T.; Ogi, Y.; Endo, T.; Tsukiyama, K.; Kuroda, H. *Jpn. J. Appl. Phys.* **2002**, *41*, 113.
(37) Tono, K.; Kondoh, H.; Hamada, Y.; Suzuki, T.; Bito, K.; Ohta, T.; Sato, S.; Hamaguchi, H.; Iwata, A.; Kuroda, H. *Jap. J. Appl. Phys.* **2005**, *44*, 7561.
(38) Bhardwaj, V. R.; Corkum, P. B.; Rayner, D. M. *Phys. Rev. Lett.* **2003**, *91*, 203004. Sahnoun, R.; Nakai, K.; Sato, Y.; Kono, H.; Fujimura, Y.; Tanaka, M. *Chem. Phys. Lett.* **2006**, *460*, 167. Sahnoun, R.; Nakai, K.; Sato, Y.; Kono, H.; Fujimura, Y.; Tanaka, M. *J. Chem. Phys.* **2006**, *125*, 184306.
(39) Murakami, M.; Tanaka, M.; Yatsuhashi, T.; Nakashima, N. *J. Chem. Phys.* **2007**, *126*, 104304. Tanaka, M.; Panja, S.; Murakami, M.; Yatsuhashi, T.; Nakashima, N. *Chem. Phys. Lett.* **2006**, *427*, 255.
(40) Kira, A.; Arai, S.; Imamura, M. *J. Phys. Chem.* **1972**, *76*, 1119.
(41) Masnovi, J. M.; Kochi, J. K.; Hilinski, E. F.; Rentzepis, P. M. *J. Phys. Chem.* **1985**, *89*, 5387.
(42) Aalbersberg, W. Ij.; Hoijtink, G. J.; Mackor, E. L.; Weijland, W. P. *J. Chem. Soc.* **1959**, 3049. Shida, T.; Hamill, W. H *J. Chem. Phys.* **1966**, *44*, 2375.
(43) Badger, B.; Brocklehurst, B. *Trans. Faraday Soc.* **1969**, *65*, 2588.
(44) Shida, T.; Iwata, S. *J. Chem. Phys.* **1972**, *56*, 2858.
(45) Donati, D.; Guarini, G. G. T.; Sarti-Fantoni, P. *Mol. Cryst. Liq. Cryst.* **1981**, *69*, 241.
(46) Yeretzian, C.; Hansen, K.; Diederich, F.; Whetten, R. L. *Nature* **1992**, *359*, 44.

JP8082985